

## Role of electric fields in the MHD evolution of the kink instability

This content has been downloaded from IOPscience. Please scroll down to see the full text.

2017 New J. Phys. 19 023034

(<http://iopscience.iop.org/1367-2630/19/2/023034>)

View [the table of contents for this issue](#), or go to the [journal homepage](#) for more

Download details:

IP Address: 89.164.198.148

This content was downloaded on 17/02/2017 at 16:20

Please note that [terms and conditions apply](#).



## PAPER

## Role of electric fields in the MHD evolution of the kink instability

Giovanni Lapenta<sup>1,3</sup> and Marina Skender<sup>2</sup><sup>1</sup> Centrum voor Plasma-Astrofysica, Departement Wiskunde, Katholieke Universiteit Leuven, Celestijnenlaan 200B, B-3001 Leuven, Belgium<sup>2</sup> Osservatorio Astronomico di Capodimonte, Istituto Nazionale di Astrofisica, Salita Moiarello 16, I-80131 Napoli, Italy<sup>3</sup> Author to whom any correspondence should be addressed.E-mail: [giovanni.lapenta@kuleuven.be](mailto:giovanni.lapenta@kuleuven.be)**Keywords:** MHD, kink instability, magnetic reconnection, self-organization, flux rope

## RECEIVED

30 December 2016

## REVISED

28 January 2017

## ACCEPTED FOR PUBLICATION

2 February 2017

## PUBLISHED

17 February 2017

Original content from this work may be used under the terms of the [Creative Commons Attribution 3.0 licence](#).

Any further distribution of this work must maintain attribution to the author(s) and the title of the work, journal citation and DOI.



## Abstract

The discovery (Bonfiglio *et al* 2005 *Phys. Rev. Lett.* **94** 145001) of electrostatic fields playing a crucial role in establishing plasma motion in the flux conversion and dynamo processes in reversed field pinches is revisited. In order to further elucidate the role of the electrostatic fields, a flux rope configuration susceptible to the kink instability is numerically studied with an MHD code. Simulated nonlinear evolution of the kink instability is found to confirm the crucial role of the electrostatic fields. A new insight is gained on the special function of the electrostatic fields: they lead the plasma towards the reconnection site at the mode resonant surface. Without this step the plasma column could not relax to its nonlinear state, since no other agent is present to perform this role. While the inductive field generated directly by the kink instability is the dominant flow driver, the electrostatic field is found to allow the motion in the vicinity of the reconnection region.

## Introduction

The question addressed in the present letter is one on the fundamental behavior of plasmas: what is the mechanism enabling motion during a topological restructuring of the magnetic field surfaces in a plasma?

It would seem natural that if the magnetic field is changing structure, the Maxwell's equations would produce an induction electric field (via Faraday's law  $\nabla \times \mathbf{E} = \partial \mathbf{B} / \partial t$ , with  $\mathbf{E}$ ,  $\mathbf{B}$  and  $t$  representing electric field, magnetic field and time, respectively) responsible for the needed motion. In an ideal (i.e. without collisions or other dissipative processes) plasma, there is an elementary relationship between electric fields and motions, governed by Ohm's law,  $\mathbf{E} = \mathbf{v} \times \mathbf{B}$ , with  $\mathbf{v}$  representing fluid velocity. The inductive electric field generated by the variation of the magnetic field can create a plasma flow directly via Ohm's law. It is worth recalling that the ideal Ohm's law can be derived from the electron momentum equation in the limit of small electron mass and no dissipations [1].

The electric field is a vector field and as any vector field it can be split in two parts. The first part is the inductive (or electromagnetic) part that is discussed above. Mathematically it is defined as the part of the electric field that is divergence free ( $\nabla \cdot \mathbf{E} = 0$ ). Its curl is given by the variation of the magnetic field. The second part is electrostatic and mathematically it is defined as the part that is curl free ( $\nabla \times \mathbf{E} = 0$ ). The source of electrostatic fields is net charge,  $\rho$ , via the Gauss theorem ( $\nabla \cdot \mathbf{E} = \rho$ ). A mathematical theorem assures that such a split between a curl-free and a div-free part always exists and is unique [2]. The  $\mathbf{E} \times \mathbf{B}$  drift has both electromagnetic and electrostatic component, respectively:

$$\mathbf{E} \times \mathbf{B} = \frac{\partial \mathbf{A}}{\partial t} \times \mathbf{B} - \nabla \varphi \times \mathbf{B}, \quad (1)$$

with  $\mathbf{A}$  and  $\varphi$  standing for vector and scalar potential, respectively.

A well known property of plasmas is their abhorrence of free charges: a free charge in plasma without fast particles is shielded within the distance called Debye length [1]. As a consequence, with the exception of surface perturbations limited within a distance proportional to the Debye length, all free charges are shielded and the

bulk of the plasma remains nearly neutral, a condition referred to in the plasma literature as plasma quasineutrality.

However, quasineutrality is still not complete neutrality. Transient situations can lead to the violation of the complete neutrality and sizeable charge build up can arise leading to electrostatic fields that are no longer localized within the Debye length of a plasma surface. So the question comes back, would a transient that is electromagnetic in nature lead only to inductive electric fields or would the electrostatic field also be present? Bonfiglio *et al* [3] presented simulation evidence to prove that during the flux conversion and dynamo processes involved in the formation of the reversed field pinche (RFP) equilibria, it is electrostatic and not inductive electric fields that play the most important role in plasma motions. More recently, Jardin *et al* [4] used the same electrostatic dynamo idea to explain the ‘magnetic flux pumping’ enabling stationary nonsawtooth ‘hybrid’ discharges in the tokamak [5].

We attempt here to investigate what role the electrostatic part of the field plays. To do so we focus on the kink instability as a paradigm for a number of processes in plasmas. Kink modes are key in space and astrophysical plasmas [6–8] and in the evolution of fusion devices [9]. For example, in the RFP fusion device [3, 10] tearing and kink modes lead to a dynamo process that sustains the poloidal flux and the field reversal. The advantage of studying a pure instability rather than considering the full RFP evolution is the relatively simpler topology that allows one to follow in detail the topological changes of the magnetic surfaces and to investigate the role of the electrostatic field in a simpler configuration. The analysis presented here focuses on a time corresponding to the overshoot of kinetic energy because the overshoot corresponds to the moment the kink instability is most active.

## Model description

We consider a simple mathematical model of a flux rope based on the textbook screw pinch [11]. The magnetic field expression in cylindrical  $(r, \theta, z)$  coordinates is:

$$B_\theta = \frac{B_0 r}{r^2 + w^2}, B_z = 1, B_r = 0 \quad (2)$$

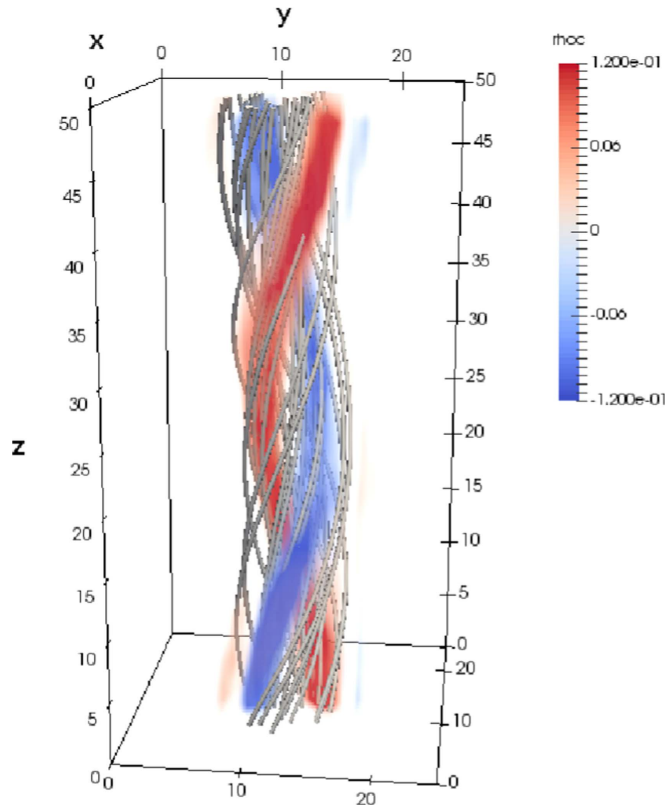
representing the helical magnetic field with helical pitch determined by the amplitude of the  $\theta$  component (i.e. by  $B_\theta$ ), with  $r$  and  $w$  radial distance and pinch radius, respectively. The magnetic field is not force free and is in balance with the plasma pressure:  $p = B_0^2 w^2 / 2\mu_0 (r^2 + w^2)^2$ , with  $\mu_0$  magnetic permeability. Since the pressure,  $p$ , is equal to  $p = \rho kT$ , with  $k$  and  $T$  Boltzmann constant and temperature, respectively, the freedom in the relative choice of the density and temperature is used to choose the temperature and density of the same profile:  $\rho = kT = \sqrt{p}$ . The plasma column is surrounded by ideal walls at a radius of  $R = 5w$ . Periodic boundary conditions are applied at the ends of the  $z$  axis ( $z = 0$  and  $z = L_z$ ). This configuration has been previously used to study the saturation of the kink mode [12] with the goal of comparing the simulated results with experimental measurements on the reconnection scaling experiment [13–15].

All simulations are carried out using the FLIP3D-MHD code [16] based on the standard visco-resistive MHD model (including the energy equation). The resistivity,  $\eta$ , is chosen according to the Spitzer’s law [17]:  $\eta = \eta_0 T^{-3/2}$ . Normalized units based on the pinch radius  $w$  and on the Alfvén speed  $v_A$  in the axial field  $B_z$  are used. To express the reference resistivity we use the Lundquist number defined as  $S = v_A w / \eta_0$  and to express the uniform viscosity we use the Reynolds number defined as  $Re = v_s w / \nu$  where  $v_s$  is the sound speed. In the run shown below,  $S = 10^3$ ,  $Re = 10^3$  and  $B_0 = 1$ .

## Results

To investigate the different influences of the inductive and electrostatic fields, specific diagnostics is introduced. The diagnostics computes the electric field and determines its divergence to compute from it the electrostatic component (figure 1). The approach as in [3] is adopted, i.e. the electrostatic part of the electric field is computed by taking the divergence of the full electric field computed from the MHD equations, and the Gauss’ law is inverted to obtain the electrostatic field.

The initial configuration is chosen to be unstable to the kink mode (i.e. the initial current exceeds the Kruskal–Shafranov limit [9]). The linear part of the evolution is found to be in good agreement with the linear theory. In the nonlinear saturation the dominant mode is at  $m = 2$  and  $n = 1$ , as it is well predicted by the so-called bubble theory [12, 18]. While the initial kink mode is ideal in nature, its nonlinear evolution and final relaxation depend crucially on resistive processes allowing reconnection of the field lines. The overall qualitative description of the kink evolution is described in textbooks [19] and has been studied previously for the same initial condition described here [12]. Figure 1 reports the final state of the system at the end of the simulation. In this study we focus entirely on the investigation of the electrostatic fields.



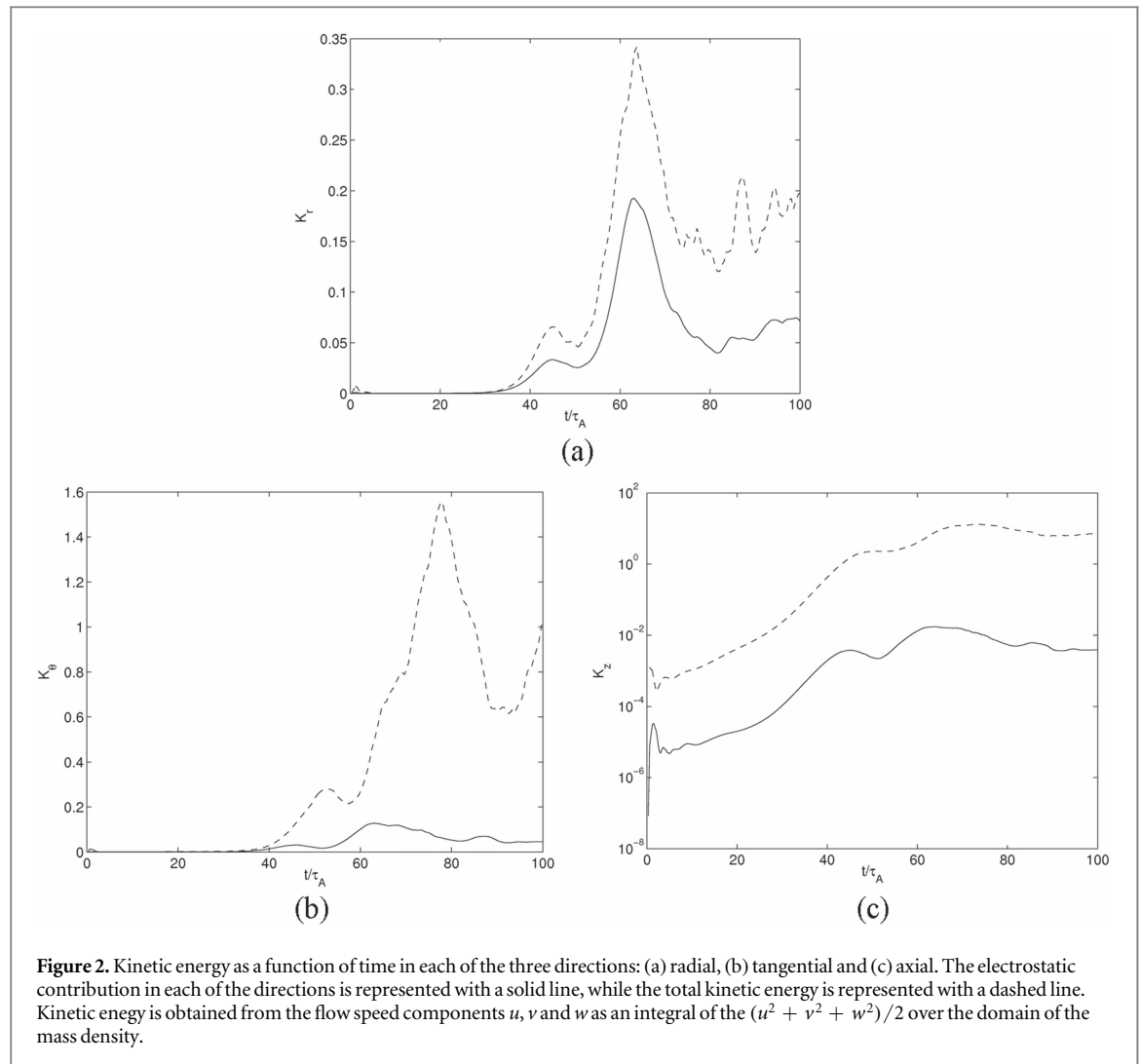
**Figure 1.** False color representation of the net charge. Gray lines represent magnetic field lines in the flux rope. Magnetic field lines are twisted and superimposed in the volume, rendering the net charge measured as  $\nabla \cdot \mathbf{E}$ .

Figure 2 presents the kinetic energy of the plasma flow generated by the kink instability as a function of time. The three components, radial, tangential and axial are presented in the three panels. For each of the components the electrostatic contribution is depicted as a solid line and the total component (sum of the inductive and electrostatic field) as a dashed line. As can be seen, in the case of the tangential and axial component, the electrostatic flow has a small contribution. For the radial flow, the electrostatic component provides a crucial contribution, being on average about 50% of the total.

The non-electrostatic component of the flow is due to the electromagnetic potential as shown by equation 1. For most of the evolution, the motion of the plasma is Alfvénic and the dominant source of the electric field is the variation of  $\mathbf{B}$  in time via Faraday's law. Still, in the radial direction, which is directly responsible for the displacement of the current off-axis, a trademark feature of the kink instability, the electrostatic field plays a significant role.

Figure 3 presents the total radial speed  $U_r$  (panel (a)), its  $(\mathbf{E} \times \mathbf{B})_r$  drift part (panel (b)) and its electrostatic component,  $-(\nabla\varphi \times \mathbf{B})_r$  (panel (c)). In the resistive Ohm's law, the resistive term  $\eta\mathbf{J}$  can itself be responsible for plasma motions. However, comparison of panels (a) and (b) of figure 3 yields evidence that this contribution is negligible. Instead, approaching the mode resonant surface, defined as the surface where the safety factor equals to the mode number [18], the electrostatic field provides basically the only contribution to the flow, as in that region  $-(\nabla\varphi \times \mathbf{B})_r$  is equal to the whole  $U_r$ .

The presence and consequences of reconnection is better appreciated if the physical quantities are shown in the  $(\theta, r)$  plane where the cylindrical geometry of the problem is straightened into a planar representation. The horizontal direction is the poloidal angle and the vertical direction is the radius. The results are shown for the central plane  $z = L_z/2$ . Figure 4 shows some relevant quantities during the phase when reconnection develops on the dominant mode resonant surface ( $m = 2, n = 1$ ). The intersection of the dominant mode resonant surface with the plane of representation is shown as a thick white curve. The helical flux surfaces are shown as thin black lines. An x-point (it is an x-line once the axial direction is considered) has formed indicative of where reconnection develops. The helical flux surfaces are pushed towards the reconnection line. As a consequence of this motion, the plasma column moves from the center outwards. Furthermore, an inverted current develops around the reconnection site to provide the resistive term needed to allow reconnection. Finally, as a byproduct of the topological change, magnetic energy is converted into heat, shown in figure 4 as regions of higher temperature in the outflow from the reconnection site.

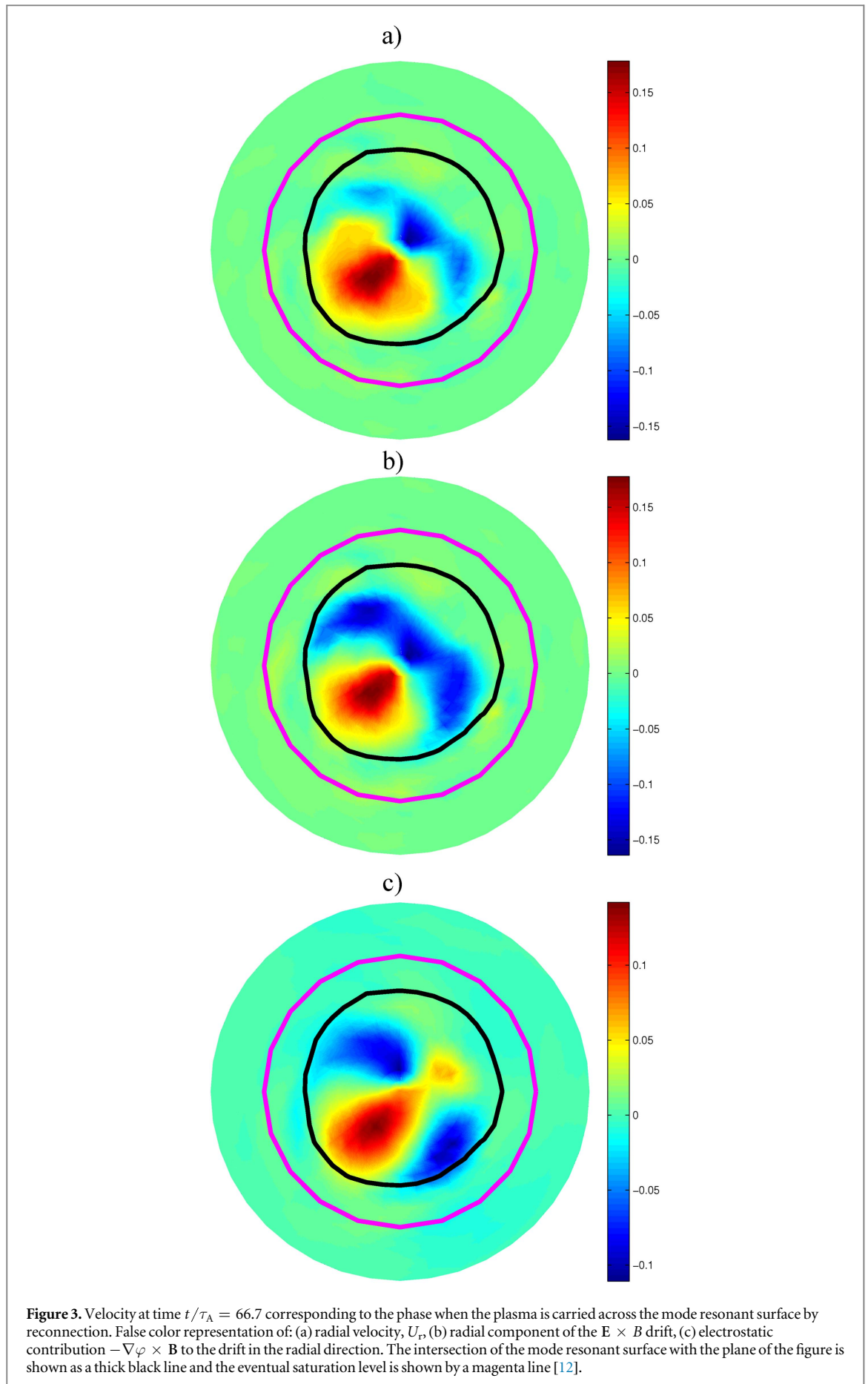


To highlight more clearly the physics in the reconnection region, figure 5 shows a composite representation of the plasma streamlines (black lines), of the helical flux surfaces (magenta lines) and of the electrostatic potential (false color). As can be observed, the streamlines drive the plasma towards the reconnection site and then away from it. In the blue and red regions corresponding to the extrema of the potential, the streamlines become equipotential, an indication that the flow is determined by the electrostatic field. But away from the reconnection site, the plasma drift becomes essentially electromagnetic. This is consistent with the outflow being essentially Alfvénic, where the inflow is at a much reduced speed. Alfvénic flows can easily create variation of the magnetic field rapid enough to create a sizeable electric field via Faraday’s law. However, slow inflows need to rely on the electrostatic field to create the needed inflow speed.

## Discussion and conclusions

The nature of the plasma flow can be electrostatic or electromagnetic or a sum of the two. Since the kink instability is a macroscopic displacement of the magnetic surface, the fundamental large scale plasma motions also have to be electromagnetic. However, the results of the above presented simulations show that while the overall motion is indeed electromagnetic in its nature, the motion of the plasma near the reconnection region is purely electrostatic. This is a rather peculiar property, the reconnection itself being an electromagnetic process in which the magnetic field is intrinsically dynamical. Since the inductive electric field is in the helical direction, normal to the plane of reconnection, the electric field needed to move the plasma in the reconnection plane towards the reconnection site is instead electrostatic.

Resistive MHD provides a macroscopic description of the electrostatic field needed to allow the motion required for the plasma to react to the kink instability. Based on the MHD, one can predict how much of the electrostatic field is needed to satisfy this macroscopic constraint. In reality, electrostatic field is created by the charge separation via the Poisson equation. While the MHD equations provide the macroscopic constraints to





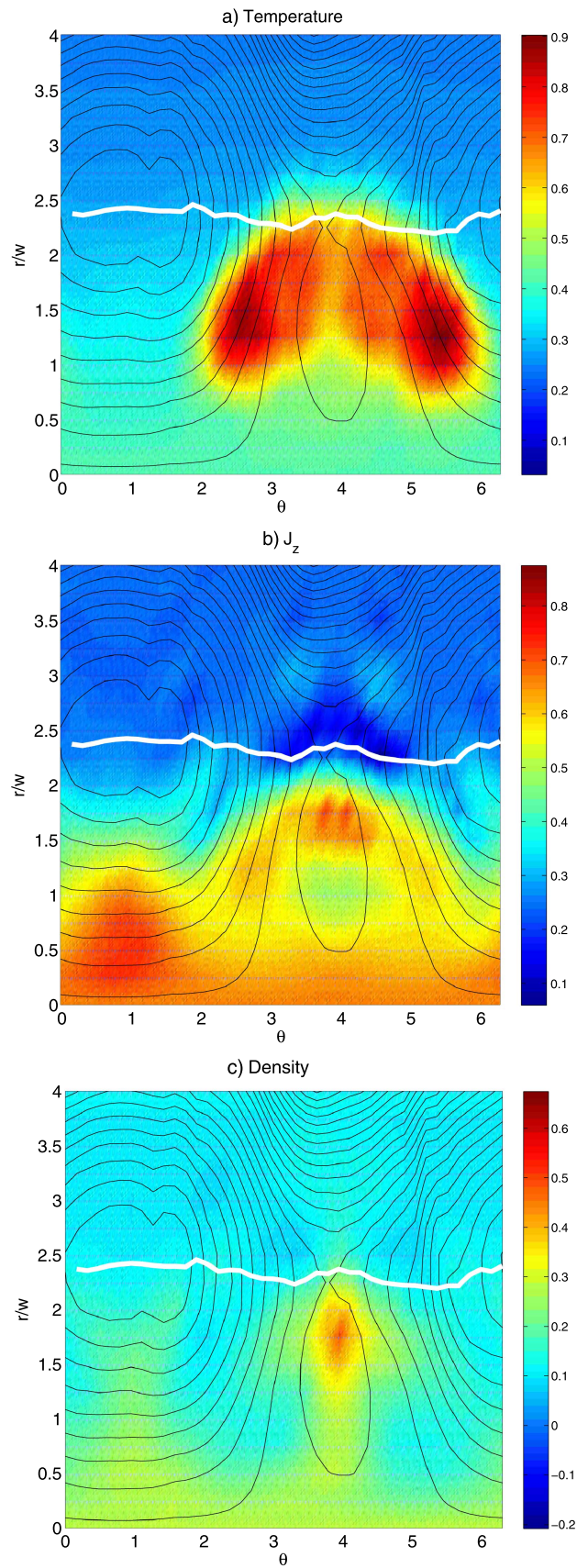


**Figure 4.** Data shown in the  $(\theta, r)$  plane at time  $t/\tau_A = 66.7$ . False color representation of: (a) temperature, (b) axial current, (c) density. The intersection of the mode resonant surface with the plane of the figure is shown as a thick white line.

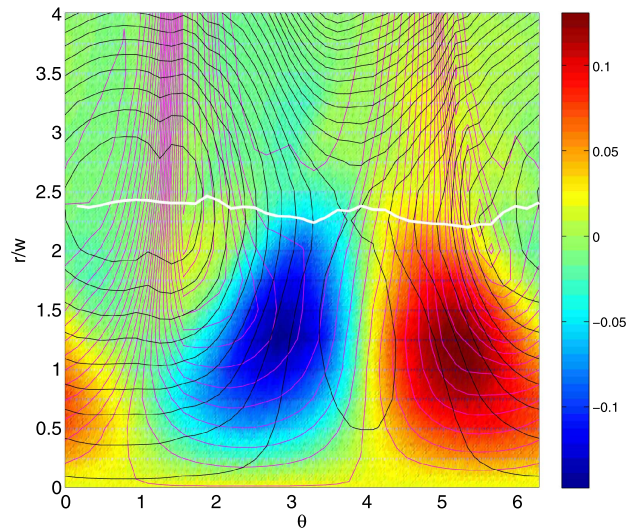


**Figure 5.** Data shown in the  $(\theta, r)$  plane at time  $t/\tau_A = 66.7$ . False color representation of the electrostatic field. The contours of the helical flux are shown in black, the streamlines of the flow are shown in magenta. The intersection of the mode resonant surface with the plane of the figure is shown as a thick white line. The region of  $\theta$  between, say, 3 and 5.5 and  $r/w$  between, say, 0 and 1.5 is dominated by the electrostatic field because the streamlines (parallel to  $\mathbf{v}$ ) run along the equipotential lines (so  $\nabla\phi$  is normal to them). The magnetic field is primarily along the  $z$ -axis, so  $\nabla\phi \times \mathbf{B}$  is parallel to  $\mathbf{v}$ .

the Poisson equation, on a smaller scale plasma has to self-organize in order to respond to such a macroscopic constraint by creating local charge separation. A fully kinetic or at least two fluid model needs to be utilized to investigate further the nature of such charge separation.

## Acknowledgments

The present work is supported by the US Air Force EOARD Project FA2386-14-1-0052, by the Onderzoeksfonds KU Leuven (Research Fund KU Leuven, GOA scheme and Space Weaves RUN project) and by the Interuniversity Attraction Poles Programme of the Belgian Science Policy Office (IAP P7/08 CHARM). This research used resources of the National Energy Research Scientific Computing Center, which is supported by the Office of Science of the US Department of Energy under Contract No. DE-AC02-05CH11231. Additional computing has been provided by NASA NAS and NCCS High Performance Computing, by the Flemish Supercomputing Center (VSC) and by PRACE Tier-0 allocations.

## References

- [1] Nicholson D R 1983 *Introduction to Plasma Theory* (New York: Wiley)
- [2] Morse P and Feshbach H 1953 *Methods of Theoretical Physics* (New York: Mc Graw-Hill)
- [3] Bonfiglio D, Cappello S and Escande D 2005 *Phys. Rev. Lett.* **94** 145001
- [4] Jardin S C, Ferraro N and Krebs I 2015 *Phys. Rev. Lett.* **115** 215001
- [5] Petty C C *et al* 2016 *Nucl. Fusion* **56** 016016
- [6] Meier D L, Koide S and Uchida Y 2001 *Science* **291** 84
- [7] Restante A L, Markidis S, Lapenta G and Intrator T 2013 *Phys. Plasmas* **20** 082501
- [8] Markidis S, Lapenta G, Delzanno G L, Henri P, Goldman M V, Newman D L, Intrator T and Laure E 2014 *Plasma Phys. Control. Fusion* **56** 064010
- [9] Wesson J 2004 *Tokamak* (Oxford: Oxford University Press)
- [10] Cappello S, Bonfiglio D and Escande D F 2006 *Phys. Plasmas* **13** 056102
- [11] Freidberg J 1987 *Ideal Magnetohydrodynamics* (New York: Plenum)
- [12] Lapenta G, Furno I and Intrator T 2006 *J. Geophys. Res.* **111** A12S06
- [13] Furno I, Intrator T, Torbert E *et al* 2003 *Rev. Sci. Instrum.* **74** 2324
- [14] Furno I, Intrator T, Lapenta G, Dorf L, Abbate S and Ryutov D 2007 *Phys. Plasmas* **14** 022103
- [15] Intrator T, Furno I, Ryutov D, Lapenta G, Dorf L and Sun X 2007 *J. Geophys. Res.* **112** A05S90
- [16] Brackbill J 1991 *J. Comput. Phys.* **96** 163
- [17] Spitzer L 1956 *Physics of Fully Ionized Gases* (New York: Interscience)
- [18] Rosenbluth M, Monticello D, Strauss H and White R 1976 *Phys. Fluids* **19** 1987
- [19] Biskamp D, Sagdeev R and Schindler K 1970 *Cosmic Electrodyn* **1** 297